

AD-A060 710

NAVAL RESEARCH LAB WASHINGTON D C
VORTEX-EXCITED UNSTEADY FORCES ON RESONANTLY VIBRATING, BLUFF S--ETC(U)

F/G 20/4

UNCLASSIFIED

NRL-MR-3820

SBIE-AD-E000 231

NL

OF |
AD
A060710



END
DATE
FILMED
01-79
DDC

2

12

AD-E000231
NRL Memorandum Report 3820

Vortex-Excited Unsteady Forces on Resonantly Vibrating, Bluff Structures

OWEN M. GRIFFIN

*Applied Mechanics Branch
Ocean Technology Division*

LEVEL II

AD A060710

DDC FILE COPY

August 1978



DDC
RECEIVED
NOV 2 1978
B

NAVAL RESEARCH LABORATORY
Washington, D.C.

Approved for public release; distribution unlimited.

78 10 05 033

ERRATA

NRL Memorandum Report 3820

p. 11 - Equation 16(b) should read

$$\varphi_1 = \text{arc tan} \left(\frac{W C_R - C_L}{C_R + W C_L} \right) \cdot$$

SECURITY CLASSIFICATION OF THIS PAGE (When Data Entered)

REPORT DOCUMENTATION PAGE		READ INSTRUCTIONS BEFORE COMPLETING FORM
1. REPORT NUMBER NRL Memorandum Report 3820	2. GOVT ACCESSION NO.	3. RECIPIENT'S CATALOG NUMBER 9
4. TITLE (and Subtitle) VORTEX-EXCITED UNSTEADY FORCES ON RESONANTLY VIBRATING, BLUFF STRUCTURES,	5. TYPE OF REPORT & PERIOD COVERED Final report, on one phase of a continuing problem.	
7. AUTHOR(s) Owen M. Griffin	6. PERFORMING ORG. REPORT NUMBER	
9. PERFORMING ORGANIZATION NAME AND ADDRESS Naval Research Laboratory Washington, D.C. 20375	8. CONTRACT OR GRANT NUMBER(s)	
11. CONTROLLING OFFICE NAME AND ADDRESS Civil Engineering Laboratory Naval Construction Battalion Center Port Hueneme, CA 93043	10. PROGRAM ELEMENT PROJECT, TASK AREA & WORK UNIT NUMBERS NRL Problem F02-36 PG 4 0009 (PDM-03)	
14. MONITORING AGENCY NAME & ADDRESS (if different from Controlling Office) 14) NRL-MR-3820	12. REPORT DATE August 1978	
16. DISTRIBUTION STATEMENT (of this Report) Approved for public release; distribution unlimited. 18) SBIE 19) AD-E000 231	13. NUMBER OF PAGES 41	
17. DISTRIBUTION STATEMENT (of the abstract entered in Block 20, if different from Report)	15. SECURITY CLASS. (of this report) UNCLASSIFIED	
18. SUPPLEMENTARY NOTES	15a. DECLASSIFICATION/DOWNGRADING SCHEDULE	
19. KEY WORDS (Continue on reverse side if necessary and identify by block number) Vortex-excited oscillations Cable strumming Fluid-structure interactions Lift forces	12) 43p.	
20. ABSTRACT (Continue on reverse side if necessary and identify by block number) This report considers recent experimental findings pertaining to the vortex-excited oscillations of bluff cylinders, and compares various approaches to measuring the resultant fluid forces. As one example, measurements of the structural damping and crossflow response amplitudes were made for several systems over a representative range of wind tunnel flow speeds. The fluid dynamic damping or reaction in-phase with the cylinder's velocity also was measured for different incident flow speeds over a range which included the locking-on of the vortex shedding to the resonant cylinder vibrations. A mathematical model is proposed in connection with these measurements, and the components (Continues)		

DD FORM 1473

1 JAN 73

EDITION OF 1 NOV 65 IS OBSOLETE

S/N 0102-014-6601

SECURITY CLASSIFICATION OF THIS PAGE (When Data Entered)

251 950

LB

20. Abstract (Continued)

of the excitation or lift force on a vibrating structure can be obtained from the model once the structural damping and fluid reaction forces are known.

In a second approach, the fluid forces were measured on a cylinder which was forced to oscillate in water at different frequencies and crossflow amplitudes over a range of incident flow speeds. Both the steady and unsteady forces are altered significantly in the locking-on regime, with large amplifications in both the lift and drag. These vortex-excited forces are then incorporated into the mathematical model for self-excited, resonant vibrations and the complementary nature of the two measurement schemes is discussed. The results obtained from the present study are suitable in general for application not only to the vortex-excited vibrations of rigid cylinders, but also to other flexible bluff structures and cables in air and in water.

CONTENTS

INTRODUCTION	1
RELATED INVESTIGATIONS	2
UNSTEADY FORCES ON RESONANTLY VIBRATING, BLUFF STRUCTURES	5
UNSTEADY FLUID FORCE MEASUREMENTS	14
ACKNOWLEDGEMENT	20
REFERENCES	21
APPENDIX I	24

ACCESSION for		
NTIS	White Section	<input checked="" type="checkbox"/>
DDC	Buff Section	<input type="checkbox"/>
UNANNOUNCED		<input type="checkbox"/>
JUSTIFICATION _____		
BY _____		
DISTRIBUTION/AVAILABILITY CODES		
Dist.	AVAIL	and/or SPECIAL
A		

VORTEX-EXCITED UNSTEADY FORCES
ON RESONANTLY VIBRATING, BLUFF STRUCTURES

INTRODUCTION

When one of the characteristic frequencies of a bluff, or unstreamlined, structure is near the frequency at which vortices are naturally shed, resonant self-excited vibrations often occur if the structure is lightly damped. There is also a range of frequencies near this so-called Strouhal frequency of shedding where forced vibrations of a bluff body cause the vortex frequency to be captured by, or to lock onto, the body frequency. This means that the body and wake oscillations have the same frequency and that the Strouhal frequency of vortex shedding from a stationary body is suppressed. This locking-on, or wake capture as it is often called, causes vortex-excited oscillations to occur over a range of flow speeds. The steady and unsteady forces which act on a structure are amplified as a result of these vibrations, and the changes in these forces are closely coupled to changes in the flow field near the body.

The purpose of this report is to consider recent experimental findings pertaining to the vortex-excited oscillations of bluff cylinders, and to compare various approaches to measuring the fluid forces. As one example, measurements of the structural damping and crossflow response amplitudes were made for several systems over a

Note: Manuscript submitted June 30, 1978.

representative range of wind tunnel flow speeds. The fluid dynamic damping, or reaction in-phase with the cylinder's velocity, also was measured for different incident flow speeds over a range which included the locking-on of the vortex shedding to the resonant cylinder vibrations. A mathematical model is proposed in connection with these measurements, and the components of the excitation or lift force on a vibrating structure can be obtained from the model once the structural damping and fluid reaction forces are known.

In another approach, the fluid forces were measured on a cylinder which was forced to oscillate in water at different frequencies and crossflow amplitudes over a range of incident flow speeds. Both the steady and unsteady forces are altered significantly in the locking-on regime, with large amplification of the lift and drag. These vortex-induced forces are then incorporated into the mathematical model for self-excited, resonant vibrations and the complementary nature of the two measurement methods is discussed. The results obtained from the present study are suitable in general for application not only to the vortex-excited vibrations of rigid cylinders, but also to other flexible bluff structures and cables in air and in water.

RELATED INVESTIGATIONS

A number of papers and reports which consider various aspects of the problem of vortex-excited oscillations and their forced-body analogues have recently appeared, as have the proceedings of a recent symposium on flow-induced structural vibrations [1]. The topics discussed at this symposium ranged from basic studies of vortex

formation and generation, to large-scale field studies of the vibrations of marine structures, and to architectural aerodynamics. For instance, Griffin & Ramberg have examined on a relatively small scale the effects of cylinder oscillations on wake similarity [2], vortex circulation and steady drag in the wakes of circular cylinders at normal and yawed incidence [3, 4, 5]. King, Prosser & Johns [6] have reported the results of laboratory-scale experiments in which they investigated both in-line and crossflow vibrations of flexible cylindrical piles in steady water currents. King [7] has also compared model experiments such as those just mentioned with full-scale experiments on offshore structures [8], and has extended his investigations to include the effects of incident flows at angles other than normal to the axis of a flexible cylinder [9].

The complexities involved in a complete formulation of the equations of fluid motion past stationary and vibrating bluff bodies still preclude a solution from first principles, and so alternative and less complicated methods have been sought for engineering applications. A formulation which couples an equation for the structural motion with a nonlinear fluid oscillator for the fluctuating lift was first proposed by Bishop & Hassan [10] and formulated with a van der Pol oscillator for the lift by Hartlen & Currie [11]. Bishop & Hassan were the first to observe that the process of locking-on involves rapid phase shifting of the unsteady fluid forces relative to the vibration displacement, and that this phase transformation is accompanied by large amplifications of both the lift and drag forces. Soon after, a modified form of this original concept which more

accurately predicted the resonant response of an elastically-mounted cylinder was proposed and compared with experiments by Skop & Griffin [12] and Griffin, Skop & Koopmann [13]. Iwan & Blevins [14] also have proposed an oscillator formulation which is based upon the integral momentum equation for a system composed of a bluff cylinder in a uniform, steady flow. These so-called non-linear or "wake-oscillator" models have been generalized by Skop & Griffin [15], Blevins & Burton [16] and Iwan [17] to include the vortex-excited oscillations of elastic structural elements. The formulations of Skop & Griffin and Iwan were arrived at independently but are identical and yield the same results for a variety of cylindrical structures such as flexible cantilevers, taut cables and pivoted, rigid members in air and water.

A wake-oscillator type of formulation recently was applied by Blake [18] to the problem of predicting the vortex-excited response of blunt-based hydrofoil struts. Good agreement was obtained for the predicted and measured modal displacement amplitudes of a cantilever strut under varying structural damping and flow conditions. This successful extension of the nonlinear oscillator concept to the case of the vortex-excited bending vibrations of hydrofoils gives further evidence of the potential importance of such methods in engineering practice.

Most recently the unsteady lift forces on vibrating cylinders were measured by Griffin & Koopmann [19] in a wind tunnel, and by Mercier [20] and Sarpkaya [21] in water tunnels. Further evidence was given in these experiments of the highly nonlinear dependence

between the various fluid dynamic force components and the amplitude and frequency of the vortex-excited and forced, resonant vibrations.

UNSTEADY FORCES ON RESONANTLY VIBRATING, BLUFF STRUCTURES

The equation of motion for a resonantly vibrating, cylindrical structure, excited by vortex shedding, can be written in the form

$$\ddot{y} + 2 \zeta_s \dot{y} + y = \mu \left(\frac{\omega_s}{\omega_n} \right)^2 (C_L - C_R) \quad (1)$$

where $(\bullet) = \frac{d}{d\tau}$. Here $y = y/D$, $\tau = \omega_n t$, $\mu = \frac{\rho D^2}{8\pi^2 S^2 M}$ and ζ_s is the

structural damping ratio. The force coefficients are

$$\text{Lift: } C_L = \frac{\bar{F}_L}{\frac{1}{2} \rho V^2 D} = C_L \sin(\alpha\tau + \varphi), \alpha = \frac{\omega}{\omega_n}, \quad (2a)$$

$$\text{Reaction: } C_R = \frac{\bar{F}_R}{\frac{1}{2} \rho V^2 D} = C_R \sin(\alpha\tau + \varphi_1), \alpha = \frac{\omega}{\omega_n}, \quad (2b)$$

as defined by Griffin and Koopmann [19], where φ and φ_1 are the phase angles between the lift and the displacement and the reaction and the acceleration, respectively. The two forces represented by C_L and C_R are orthogonal, as will be shown later. An analogous formulation of the equation of motion recently has been introduced by Blake, Maga & Finkelstein [22], who investigated the vortex-excited oscillations of propellers and hydrofoils.

If the displacement y is written as

$$y = Y \sin \alpha \tau, \quad \alpha = \frac{\omega}{\omega_n} \quad (3)$$

then the equation of motion separates into

$$\sin \alpha \tau: -\alpha^2 Y + Y - \mu \left(\frac{\omega_s}{\omega_n} \right)^2 \left[C_L \cos \varphi - C_R \cos \varphi_1 \right] = 0 \quad (4a)$$

and

$$\cos \alpha \tau: 2 \zeta_s Y - \mu \left(\frac{\omega_s}{\omega_n} \right)^2 \left[C_L \sin \varphi - C_R \sin \varphi_1 \right] = 0 \quad (4b)$$

when the coefficients of $\sin \alpha \tau$ and $\cos \alpha \tau$ are grouped appropriately.

The various force components are identified as follows

STRUCTURAL	FLUID
INERTIA	INERTIA
+ STIFFNESS	ADDED MASS
- $\alpha^2 Y$	+ $Y = \mu \left(\frac{\omega_s}{\omega_n} \right)^2 \left[C_L \cos \varphi - C_R \cos \varphi_1 \right]$
+ $2 \zeta_s Y$	FLUID
= $\mu \left(\frac{\omega_s}{\omega_n} \right)^2$	EXCITATION
	DAMPING
	+ $\left[C_L \sin \varphi - C_R \sin \varphi_1 \right]$

Using a different notation Sarpkaya [21] has expressed the measured fluid force on a vibrating cylinder as the sum of orthogonal components in the form

$$C_{TOTAL} = \frac{\bar{F}}{\frac{1}{2} \rho V^2 D} = C_{mh} \sin \alpha \tau - C_{dh} \cos \alpha \tau, \quad (5)$$

where C_{mh} is an "inertia" force and C_{dh} is a "drag" force. These

force components are related to Sarpkaya's "generalized Morison coefficients" C_{dl} and C_{ml} by

$$C_{dh} = \frac{8}{3\pi} C_{dl} \left(2 \pi \frac{\bar{y}}{D} \right)^2 V_r^{-2} \quad (6a)$$

and

$$C_{mh} = \pi^2 C_{ml} \left(2 \pi \frac{\bar{y}}{D} \right)^2 V_r^{-2} \quad (6b)$$

where V_r is the "reduced velocity" $V_r = \frac{2\pi V}{\omega_n D}$.

In this case the equation of motion for the cylinder is written as

$$\ddot{y} + 2 \zeta_s \dot{y} + y = \mu \left(\frac{\omega}{\omega_n} \right)^2 \left[C_{mh} \sin \alpha \tau - C_{dh} \cos \alpha \tau \right]. \quad (7)$$

(The drag force C_{dh} is negative when energy is transferred to the cylinder, as is the case for resonant, vortex-excited oscillations.)

If a steady-state response is assumed, then

$$y = Y \sin (\alpha \tau - \epsilon),$$

where ϵ is an undefined phase angle. This equation of motion then separates into

$$\begin{aligned} \sin \alpha \tau: \quad & \alpha^2 Y \cos \epsilon + 2 \zeta_s Y \sin \epsilon + Y \cos \epsilon \\ & - \mu \left(\frac{\omega}{\omega_n} \right)^2 C_{mh} = 0 \end{aligned} \quad (8a)$$

and

$$\begin{aligned} \cos \alpha \tau: \quad & \alpha^2 Y \sin \epsilon + 2 \zeta_s Y \cos \epsilon - Y \sin \epsilon \\ & + \mu \left(\frac{\omega}{\omega_n} \right)^2 C_{dh} = 0 \end{aligned} \quad (8b)$$

when the coefficients of $\sin \alpha \tau$ and $\cos \alpha \tau$ are again grouped appropriately. If the first equation is multiplied by $\sin \epsilon$ and the second by $\cos \epsilon$, then

$$2 \alpha \zeta_s Y - \mu \left(\frac{\omega_s}{\omega_n} \right)^2 \left[C_{mh} \sin \epsilon - C_{dh} \cos \epsilon \right] = 0 \quad (9a)$$

when the two results are added. Next, equation (8a) is multiplied by $\cos \epsilon$ and equation (8b) by $\sin \epsilon$, to obtain

$$- \alpha^2 Y + Y - \mu \left(\frac{\omega_s}{\omega_n} \right)^2 \left[C_{mh} \cos \epsilon + C_{dh} \sin \epsilon \right] = 0 \quad (9b)$$

when the two equations are subtracted. The terms in equations (9a) and (9b) can be arranged and labeled in the same manner as before:

STRUCTURAL INERTIA	+	STRUCTURAL STIFFNESS	=	$\mu \left(\frac{\omega_s}{\omega_n} \right)^2$	FORCE TERMS	$\left[C_{dh} \sin \epsilon + C_{mh} \cos \epsilon \right]$
-----------------------	---	-------------------------	---	--	----------------	--

STRUCTURAL DAMPING	=	$\mu \left(\frac{\omega_s}{\omega_n} \right)^2$	FORCE TERMS	$\left[- C_{dh} \cos \epsilon + C_{mh} \sin \epsilon \right]$
-----------------------	---	--	----------------	--

These equations have the same form as those formulated by Griffin & Koopmann [19], and the two approaches are in fact identical when

$$C_L \sin \varphi = -C_{dh} \cos \epsilon, \quad \text{EXCITATION}^+ \quad (10a)$$

$$C_L \cos \varphi = C_{dh} \sin \epsilon, \quad \text{FLUID INERTIA} \quad (10b)$$

$$C_R \sin \varphi_1 = -C_{mh} \sin \epsilon, \quad \text{FLUID REACTION (DAMPING)} \quad (10c)$$

$$C_R \cos \varphi_1 = -C_{mh} \cos \epsilon, \quad \text{ADDED MASS} \quad (10d)$$

⁺See Appendix I for a further discussion of these equations.

These relations can be used to compare results from the two approaches.

From the above system of equations it follows that $\tan \varphi_1 = \tan \epsilon$ and

$$\tan \varphi = - \frac{1}{\tan \epsilon} = - \frac{1}{\tan \varphi_1} . \quad (11)$$

(Recall that ϵ and φ are measured from y , whereas φ_1 is measured from \ddot{y} .) It also follows from these equations that

$$C_L^2 = C_{dh}^2, \text{ or } |C_L| = |C_{dh}|,$$

and that

$$C_R^2 = C_{mh}^2, \text{ or } |C_R| = |C_{mh}|.$$

The phase relations between the various forces components are shown in Figure 5(b) for a typical set of conditions.

A relation between the displacement Y and the total fluid force can be obtained by squaring and adding equations (4a) and (4b) to yield

$$\begin{aligned} (1 - \alpha^2)^2 + (2 \alpha \zeta_s)^2 Y^2 = \mu^2 \left(\frac{\omega_s}{\omega_n} \right)^4 & \left[C_L^2 + C_R^2 \right. \\ & \left. - 2 C_L C_R (\cos \varphi \cos \varphi_1 + \sin \varphi \sin \varphi_1) \right]. \end{aligned}$$

This equation simplifies to

$$\left[(1 - \alpha^2)^2 + (2 \zeta_s \alpha)^2 \right] Y^2 = \mu^2 \left(\frac{\omega_s}{\omega_n} \right)^4 \left[C_L^2 + C_R^2 \right] \quad (12)$$

since $\tan \varphi = - \frac{1}{\tan \varphi_1}$. The phase angles φ and φ_1 can be retrieved from the equations

$$2 \zeta_s Y = \mu \left(\frac{\omega_s}{\omega_n} \right)^2 C_T \left[\frac{C_L}{C_T} \sin \varphi - \frac{C_R}{C_T} \sin \varphi_1 \right],$$

$$(1 - \alpha^2) Y = \mu \left(\frac{\omega_s}{\omega_n} \right)^2 C_T \left[\frac{C_L}{C_T} \cos \varphi - \frac{C_R}{C_T} \cos \varphi_1 \right],$$

where

$$C_T = \sqrt{C_L^2 + C_R^2}.$$

Also choose $\varphi_1 - \varphi = \pi/2$, so that these equations reduce to

$$2 \alpha \zeta_s Y = \mu \left(\frac{\omega_s}{\omega_n} \right)^2 C_T [-\sin \beta \cos \varphi_1 - \cos \beta \sin \varphi_1]$$

and

$$(1 - \alpha^2) Y = \mu \left(\frac{\omega_s}{\omega_n} \right)^2 C_T [+ \sin \beta \sin \varphi_1 - \cos \beta \cos \varphi_1]$$

where $\beta = \arctan \frac{C_L}{C_R}$. Simplifying further, one obtains the equations

$$- \mu \left(\frac{\omega_s}{\omega_n} \right)^2 C_T \sin(\varphi_1 + \beta) = 2 \alpha \zeta_s Y, \quad (13a)$$

$$- \mu \left(\frac{\omega_s}{\omega_n} \right)^2 C_T \cos(\varphi_1 + \beta) = (1 - \alpha^2) Y, \quad (13b)$$

and

$$\tan(\varphi_1 + \beta) = \frac{2 \alpha \zeta_s}{(1 - \alpha^2)} = W. \quad (13c)$$

This latter equation can be rearranged as

$$\tan \varphi_1 = \frac{W - \tan \beta}{1 + W \tan \beta}. \quad (13d)$$

If $W = \tan \gamma$, then

$$\tan \varphi_1 = \tan(\gamma - \beta) \quad (14a)$$

and

$$\varphi_1 = \gamma - \beta. \quad (14b)$$

The tangents of the various phase angles are

$$\tan \varphi_1 = \frac{-\left(\frac{C_L}{C_R}\right) + W}{1 + W \frac{C_L}{C_R}} = \frac{-C_L + W C_R}{C_R + W C_L} \quad (15a)$$

$$\tan \varphi = -\frac{1}{\tan \varphi_1} = \frac{C_R + W C_L}{C_L - W C_R} \quad (15b)$$

or, alternately, the angles φ and φ_1 are

$$\varphi = \arctan \left(\frac{C_R + W C_L}{C_L - W C_R} \right). \quad (16a)$$

$$\varphi_1 = \arctan \left(\frac{C_L + W C_R}{C_R + W C_L} \right). \quad (16b)$$

according to the formulation of Griffin & Koopmann [1].

Similar expressions can be found from the formulation employed by Sarpkaya [21] and his students [see Raposo [23], Meyers [24] and Fortik [25]]. The equations of motion reduce to

$$2 \alpha \zeta_s \gamma = \mu \left(\frac{\omega_s}{\omega_n} \right)^2 C_T \left[\frac{C_{mh}}{C_T} \sin \epsilon - \frac{C_{dh}}{C_T} \cos \epsilon \right],$$

and

$$(1 - \alpha^2) \gamma = \mu \left(\frac{\omega_s}{\omega_n} \right)^2 C_T \left[\frac{C_{mh}}{C_T} \cos \epsilon + \frac{C_{dh}}{C_T} \sin \epsilon \right],$$

where

$$C_T = \sqrt{C_{mh}^2 + C_{dh}^2}.$$

If $\sin \beta' = \frac{C_{dh}}{C_T}$, and $\cos \beta' = \frac{C_{mh}}{C_T}$, then these equations become

$$2 \alpha \zeta_s Y = \mu \left(\frac{w_s}{w_n} \right)^2 C_T \sin (\epsilon - \beta') \quad (17a)$$

$$(1 - \alpha^2) Y = \mu \left(\frac{w_s}{w_n} \right)^2 C_T \cos (\epsilon - \beta') \quad (17b)$$

which yield the result

$$\tan (\epsilon - \beta') = \frac{2 \alpha \zeta_s Y}{(1 - \alpha^2) Y} = \frac{2 \alpha \zeta_s}{(1 - \alpha^2)} = W. \quad (17c)$$

This equation can be rearranged as

$$\tan \epsilon = \frac{W + \tan \beta'}{1 - W \tan \beta'}. \quad (18)$$

If $W = \tan \gamma$ as before, then

$$\epsilon = \gamma + \beta',$$

where

$$\beta' = \arctan \left(\frac{C_{dh}}{C_{mh}} \right) \quad (19a)$$

and

$$\gamma = \arctan \left(\frac{2 \alpha \zeta_s}{1 - \alpha^2} \right). \quad (19b)$$

In order for self-excited oscillations to take place, energy must be transferred to the cylinder and its mounting system from the fluid.

The energy transfer \bar{E}^+ over a cycle of the oscillation is given by the integral

$$\bar{E} = \int_0^T \bar{F}_L d\bar{y} = \int_0^T \bar{F}_L \dot{\bar{y}} dt \quad (20)$$

The lift force is, in Sarpkaya's notation,

$$\bar{F}_L = -C_{dh} (1/2 \rho V^2 D L) \cos \alpha \tau,$$

+ See Appendix I for a further discussion of the work done and energy dissipated by the various forces over a cycle of the cylinder motion.

and the cylinder vibration velocity is

$$\dot{y} = \alpha Y D \cos (\alpha \tau - \epsilon),$$

so that the equation for the energy transfer is

$$\bar{E} = \frac{1}{2} \rho V^2 D^2 L \int_0^{\omega_n T} (-C_{dh}) \cos \alpha \tau (Y \alpha) \cos (\alpha \tau - \epsilon) d\tau$$

or

$$E = \frac{\bar{E}}{\frac{1}{2} \rho V^2 D^2 L} = (-C_{dh}) Y \int_0^{2\pi} \cos u \cos (u - \epsilon) du,$$

$$= \pi (-C_{dh}) Y \cos \epsilon. \quad (21a)$$

A necessary condition for self-excited oscillations to take place is

$$E = \pi (-C_{dh}) Y \cos \epsilon > 0$$

or, equivalently, $\cos \epsilon > 0$ since $-C_{dh}$ is positive. This leads to the condition

$$C_{mh} - W C_{dh} > 0 \quad (21b)$$

for self-excited oscillations since

$$\cos \epsilon = \frac{C_{mh} - W C_{dh}}{\sqrt{(C_{mh} - W C_{ch})^2 + (C_{dh} + W C_{mh})^2}}.$$

In the notation adopted by Griffin & Koopmann [19], the energy transfer is

$$\bar{E} = 1/2 \rho V^2 D^2 L \int_0^{\omega_n T} C_L \sin (\alpha \tau + \varphi) (Y \alpha) \cos \alpha \tau d\tau$$

or

$$E = C_L Y \int_0^{2\pi} \sin (u + \varphi) \cos u du = \pi C_L Y \sin \varphi. \quad (22)$$

Since C_L is positive, a necessary condition for self-excited oscillations is $\sin \varphi > 0$. This leads to the condition

$$C_R + W C_L > 0$$

since

$$\sin \varphi = \frac{C_R + W C_L}{\sqrt{(C_R + W C_L)^2 + (C_L - W C_R)^2}}$$

This is analogous to the condition derived between C_{mh} and C_{dh} .

UNSTEADY FLUID FORCE MEASUREMENTS

Some interesting and useful comparisons can be made between the fluid forces measured when a cylinder is forced to vibrate and the fluid forces measured when the cylinder is resonantly excited by vortex shedding. The forced cylinder measurements discussed here were made by Sarpkaya [21] and Mercier [20], and the self-excited cylinder measurements were made by Griffin & Koopmann [19] and others [26, 27, 28].

Typical examples of the measurements reported by Sarpkaya are shown in Figures 1 and 2. The measured values for the inertia coefficient C_{mh} are shown in Figure 1 as a function of the reduced velocity V_r , for a displacement amplitude of $Y = 0.50$. Of particular note is the rapid change in C_{mh} in the vicinity of $V_r = 5$. This effect corresponds to the onset of locking-on between the vortex and vibration frequencies when the characteristic frequency of the flow approaches the vibration frequency. The drag or resistance force C_{dh} is plotted in Figure 2 as a function of V_r at the same displacement amplitude, $Y = 0.50$. This component of the total fluid dynamic

force becomes negative near $V_r = 5$. The terminology employed by Sarpkaya is somewhat unwieldy and is an extension of his previous work [29] with the so-called Morison equation [30] for purely periodic flow past stationary cylinders. In effect, C_{dh} is the negative of the lift coefficient as it is usually characterized, so that the negative value of C_{dh} near $V_r = 5$ suggests a net transfer of energy to the cylinder in that region. These forced-cylinder results can be compared to the vortex-excited, transverse oscillations of structures which typically occur in the range $V_r = 4.5$ to 8 when the damping of a structure is sufficiently small [19, 26, 31].

The excitation component of the lift force $C_L \sin \phi = -C_{dh} \cos \epsilon$ measured by Griffin & Koopmann [19] is plotted in Figure 3 for two cases. For the first case, termed System I, the cylinder reached a maximum displacement amplitude of $Y = 0.47$, while for the second case the maximum displacement was $Y = 0.27$. The conditions for these experiments are listed in Table 1. The lift force coefficients in Figure 3 were deduced from structural and fluid dynamic damping or reaction forces on freely-vibrating cylinders in a wind tunnel. A typical example of the fluid dynamic damping ratio ζ_F as a function of the reduced velocity V_r is shown in Figure 4. There is a marked decrease in the damping in the region of the locking-on, and much the same effect has been observed by Blake, Maga & Finkelstein [22] during measurements of the vortex-excited bending vibrations of blunt-based hydrofoil models.

A comparison now will be made between the force components of Sarpkaya's forced vibration experiments and the vortex-excited forces.

Consider as an example the measurements $C_{mh} = -0.5$ and $C_{dh} = -0.2$ at $V_r = 5.5$ and $Y = 0.25$, reported by Sarpkaya [21], and assume $W = 0.05$ as a typical value [see reference 19]. For this case $\epsilon = 204.7^\circ$ and

$$C_{mh} - W C_{dh} = -0.5 - 0.05 (-0.2) = -0.49,$$

so that self-excited oscillations do not take place (see equation 21b).

A phase diagram of the various force components is shown as Case 1 in Figure 5(a). As an additional example consider a set of conditions such that $C_{mh} = 1.6$ and $C_{dh} = -0.9$ at $V_r = 5$ and $Y = 0.5$. Assuming once again for convenience that $W = 0.05$, then $\epsilon = -26.5^\circ$ and

$$C_{mh} - W C_{dh} = 1.6 - 0.05 (-0.9) = 1.64,$$

so that self-excited oscillations are possible for these conditions.

This is shown as Case 2 in Figure 5(b).

The excitation component of the lift force is defined as

$$C'_L = C_L \sin \phi = -C_{dh} \cos \epsilon \quad (10a)$$

and is important from the standpoint of energy transfer to the vibrating structure. The measurements made by Sarpkaya can be compared to the measurements of other investigators by means of the above equation. The maximum value of the force coefficient $-C_{dh}$ in Figure 2 occurs at $V_r = 5$, and the same result is obtained at the displacement amplitudes $Y = 0.13, 0.25$ and 0.75 [21]. The several values of $-C_{dh}$ and C_{mh} are listed in Table 2 together with the related values of the force components $-C_{dh} \cos \epsilon$. For all of these cases of forced vibration the condition for self-excitation

$$C_{mh} - W C_{dh} > 0$$

is satisfied, thus assuring the possibility of the equivalent vortex-

excited oscillation. The results for $-C_{dh} \cos \epsilon$ are plotted against the peak displacement in Figure 6 together with a host of similar findings from the results obtained by other investigators. The conditions under which the experiments were performed are described in Table 3.

Mercier [20] measured the force coefficients C_{mh} and C_{dh} on a cylinder which was forced to vibrate in water. These measurements were not nearly as extensive and precise as were those of Sarpkaya, but it is possible to estimate the various force components given by equations (10a to c) from Mercier's published data. The results are listed in Table 2(b) and are plotted in Figures 6 and 7. The minimum value of C_{dh} was measured once again at $V_r = 5.5-6$, and for all of the cases listed in Table 2(b) the condition

$$C_{mh} - W C_{dh} > 0$$

was satisfied. The estimated force coefficients $-C_{dh} \cos \epsilon$ from Mercier's measurements are in reasonably good agreement with the other results plotted in Figure 6. All of the lift force measurements in the figure exhibit the nonlinear dependence upon amplitude that is characteristic of vortex-excited oscillations. This nonlinear "wake-oscillator" was first observed by Bishop & Hassan [10], and has since been studied in considerable detail by others [11, 12, 14].

The measured vortex-excited displacements in Figure 6 are scaled by the modal response factor

$$I_1^{\frac{1}{2}} |\psi_1(x)|$$

which takes account of the normal modes $\psi_1(x)$ of a flexible structure

of immersed length L . As shown by Skop & Griffin [15] and Iwan [17],

$$I_i = \frac{\int_0^L \psi_1^4(x) dx}{\int_0^L \psi_1^2(x) dx} \quad (23)$$

For the special case of a circular cylinder $|\psi_1(x)| = I_i = 1$, and the corresponding values for cantilevers and pivoted rods are listed in reference 31.

Several important characteristics of the lift force behavior during locking-on are clear from the results plotted in Figure 6. First, there is a maximum of the excitation component of the lift force at a peak-to-peak displacement between 0.6 and 1 diameters for all of the cases shown in the figure. Second, the maximum of the lift coefficient is approximately $C'_L = 0.5$ to 0.6 for most cases, a notable exception being Sarpkaya's result, $C'_L = 0.75$. The excitation force coefficient C'_L decreases to zero at displacement amplitudes near $Y = 1$, and this results in a limiting amplitude of vortex-excited oscillation of one to one and one-half diameters. Sarpkaya's measurements give convincing evidence of this limit, since in his water tunnel experiments with forced cylinders the sign of the force coefficient C_{dh} changed from negative to positive as the vibration displacement was increased from 0.75 diameters to 1.03 diameters. Mercier [20] also observed a change in the sign of the force coefficient C_{dh} as the vibration displacement \bar{y} was increased to 1.3 diameters from the values listed in Table 2(b).

The formulations for the fluid dynamic forces due to vortex shedding introduced by Blake, Maga & Finkelstein [22] and Griffin &

Koopmann [19] are based on the hypothesis that both flow-induced lift (excitation) and reaction (damping) forces act on a resonantly vibrating, bluff structure. The fluid damping forces were measured in air by Griffin & Koopmann, see Figure 4, and in water by Blake and his colleagues, and the lift coefficient was obtained by equating the lift component $C_L \sin \varphi$ to the sum of the structural damping and fluid reaction forces as given by equation (10a).

It is possible to deduce the damping or reaction effect of the fluid from Sarpkaya's total force coefficients by means of equation (10c),

$$C_R \sin \phi_1 = -C_{mh} \sin \epsilon,$$

as a further step in comparing the two approaches described in the previous section. The results are listed in Table 2(a) and are plotted in Figure 7, and they yield further evidence that the fluid force decomposition described by equations (10a) through (10d) is an appropriate one. A comparison between the force components deduced from Sarpkaya's forced-vibration measurements of C_{mh} and C_{dh} and plotted in Figures 6 and 7 shows that the excitation and reaction forces are very nearly equal. Though Mercier's force measurements were not as extensive as those of Sarpkaya, it is possible to estimate the reaction effect of the fluid from his faired curves of C_{mh} and C_{dh} . The results are listed in Table 2(b) and plotted in Figure 7. The same reaction or damping forces component as reported by Griffin & Koopmann is plotted in Figure 7, and all of the measurements show the same general pattern of behavior even though these latter experiments were performed in a wind tunnel.

It is important to remark upon the complementary nature of the two approaches just described for measuring the vortex-excited forces on bluff bodies. For instance, the Morison-type force coefficients C_{mh} and C_{dh} , as obtained from a Fourier decomposition of the total force measured by driving the cylinder, do not give the necessary detailed picture of the various force components which act due to resonant, vortex-excited oscillations. On the other hand, it is an exceedingly difficult experimental undertaking to measure the resultant fluid dynamic force on a resonantly vibrating, self-excited bluff cylinder. Only the fluid damping, structural damping and added mass components of the total force system are conveniently measured in this latter case. Thus, in applying the results from the two approaches just discussed, it is necessary to recognize the limitations inherent in each and to take advantage of their complementary nature in solving problems associated with the vortex-excited vibrations of bluff structures.

ACKNOWLEDGEMENT

This report has been prepared as part of the research program of the Naval Research Laboratory and is published by permission. The support of the Civil Engineering Laboratory, Naval Construction Battalion Center is gratefully acknowledged.

REFERENCES

1. E. Naudascher, ed., Flow-Induced Structural Vibrations, Berlin: Springer-Verlag (1974).
2. O.M. Griffin, "A Universal Strouhal Number for the 'Locking-on' of Vortex Shedding to the Vibrations of Bluff Cylinders," *Journal of Fluid Mechanics*, Vol. 85, 591-606 (1978).
3. O.M. Griffin & S.E. Ramberg, "The Vortex-Street Wakes of Vibrating Cylinders," *Journal of Fluid Mechanics*, Vol. 66, 553-576 (1974).
4. O.M. Griffin & S.E. Ramberg, "On Vortex Strength and Drag in Bluff Body Wakes," *Journal of Fluid Mechanics*, Vol. 69, 721-728 (1975).
5. S.E. Ramberg, "The Influence of Yaw Angle Upon the Vortex Wakes of Stationary and Vibrating Cylinders," Ph.D. Thesis, Catholic University of America (April 1978).
6. R. King, M. Prosser & D.J. Johns, "On Vortex Excitation of Model Piles in Water," *Journal of Sound and Vibration*, Vol. 29, 169-188 (1973).
7. R. King, "Vortex-Excited Structural Oscillations of a Circular Cylinder in Steady Currents," Offshore Technology Conference Preprint 1948 (1974).
8. L.R. Wootton, M.H. Warner, R.M. Sainsbury & D.H. Cooper, *Oscillation of Piles in Marine Structures*, Construction Industry Research and Information Association: London, CIRIA Report 41 (1972).
9. R. King, "Vortex Excited Oscillations of Yawed Circular Cylinders." *Transactions of the ASME, Series I, Journal of Fluids Engineering*, Vol. 99, 495-502 (1977).
10. R.E.D. Bishop & A.Y. Hassan, "The Lift and Drag Forces on a Circular Cylinder Oscillating in a Flowing Fluid," *Proceedings of the Royal Society (London) Series A*, Vol. 277, 51-75 (1964).
11. R.T. Hartlen & I.G. Currie, "A Lift-Oscillator Model for Vortex-Induced Vibrations," *Proceedings of the ASCE, Journal of Engineering Mechanics*, Vol. 69, 577-591 (1970).
12. R.A. Skop & O.M. Griffin, "A Model for the Vortex-Excited Resonant Response of Bluff Cylinders," *Journal of Sound and Vibration*, Vol. 27, 225-233 (1973).
13. O.M. Griffin, R.A. Skop & G.H. Koopmann, "The Vortex-Excited Resonant Vibrations of Circular Cylinders," *Journal of Sound and Vibration*, Vol. 31, 235-249 (1973).

14. W.D. Iwan & R.D. Blevins, "A Model for Vortex Induced Oscillation of Structures," *Transactions of the ASME, Series E, Journal of Applied Mechanics*, Vol. 41, 581-586 (1974).
15. R.A. Skop & O.M. Griffin, "On a Theory for the Vortex-Excited Oscillations of Flexible Cylindrical Structures," *Journal of Sound and Vibration*, Vol. 41, 263-274 (1975).
16. R.D. Blevins & T.E. Burton, "Fluid Forces Induced by Vortex Shedding," *Transactions of the ASME, Series I, Journal of Fluids Engineering*, Vol. 98, 19-26 (1976).
17. W.D. Iwan, "The Vortex Induced Oscillation of Elastic Structural Elements," *Transactions of the ASME, Series B, Journal of Engineering for Industry*, Vol. 97, 1378-1382 (1975).
18. W.K. Blake, "Periodic and Random Excitation of Streamline Structures by Trailing-Edge Flows," in Proc. Symposium on Turbulence in Liquids, University of Missouri, Rolla (1975).
19. O.M. Griffin & G.H. Koopmann, "The Vortex-Excited Lift and Reaction Forces on Resonantly Vibrating Cylinders," *Journal of Sound and Vibration*, Vol. 54, 435-448 (1977).
20. J.A. Mercier, "Large Amplitude Oscillations of a Circular Cylinder in a Low-Speed Stream," Ph.D. Thesis, Stevens Institute of Technology, Hoboken, New Jersey (1973).
21. T. Sarpkaya, "Transverse Oscillations of a Circular Cylinder in Uniform Flow," Naval Postgraduate School Report NPS-69SL77071-R (December 1977); see also Preprint 2921, ASCE Fall Convention and Exhibit (October 1977).
22. W.K. Blake, L.J. Maga & G. Finkelstein, "Hydroelastic Variables Influencing Propellor and Hydrofoil Singing," in Noise and Fluids Engineering, R. Hickling (ed.), ASME: New York, 191-199 (1977).
23. P.A. Raposo, "Transverse Oscillations of a Cylinder in Uniform Flow," M.S. Thesis, Naval Postgraduate School, Monterey, California (June 1976).
24. D.W. Meyers, "Transverse Oscillations of a Cylinder in Uniform Flow," M.S. Thesis, Naval Postgraduate School, Monterey, California (December 1975).
25. D.F. Fortik, "Forced Oscillations of a Cylinder in Uniform Flow," M.S. Thesis, Naval Postgraduate School, Monterey, California (June 1976).

26. R. King, "An Investigation of the Criteria Controlling Sustained Self-Excited Oscillations of Cylinders in Flowing Water," in Proc. Symposium on Turbulence in Liquids, University of Missouri, Rolla, (1977).
27. B.J. Vickery & R.D. Watkins, "Flow Induced Vibrations of Cylindrical Structures," in Proceedings of the First Australasian Conference on Hydro-mechanics (1962).
28. R.T. Hartlen, W.D. Baines & I.G. Currie, "Vortex-Excited Oscillations of a Circular Cylinder," University of Toronto Report UTME-TP-6809 (November 1968).
29. T. Sarpkaya, "In-Line and Transverse Forces on Cylinders in Oscillatory Flow at High Reynolds Numbers," Journal of Ship Research, Vol. 21, 200-216 (1977).
30. J.R. Morison, M.P. O'Brien, J.W. Johnson & S.A. Schaaf, "The Force Exerted by Surface Waves on Piles," Petroleum Transactions, Vol. 189, 149-157 (1950).
31. O.M. Griffin, R.A. Skop & S.E. Ramberg, "The Resonant, Vortex-Excited Vibrations of Structures and Cable Systems," Offshore Technology Conference Preprint 2319 (1975).

APPENDIX I

It is useful to consider the work done and the energy dissipated over a cycle of the cylinder's oscillation by the various forces in equations (1) and (7). The work and energy dissipation are given by the well-known equation

$$\Delta \bar{E} = \bar{W} = \int_0^T \bar{F} d\bar{y} = \int_0^T \bar{F} \frac{d\bar{y}}{dt} dt. \quad (A1)$$

Employing the nomenclature introduced earlier, and evaluating this integral for the structural and fluid dynamic forces in equation (1), one obtains

$$2 \zeta_s \int_0^{\omega_n T} (\dot{y})^2 d\tau = \mu \left(\frac{\omega_s}{\omega_n} \right)^2$$

$$\left\{ \int_0^{\omega_n T} C_L \sin(\alpha \tau + \varphi) \dot{y} d\tau - \int_0^{\omega_n T} C_R \sin(\alpha \tau + \varphi_1) \dot{y} d\tau \right\}.$$

The structural inertia and stiffness terms are conservative and do no net work over a cycle of the oscillation. The structural velocity \dot{y} is

$$\dot{y} = \alpha Y \cos(\alpha \tau),$$

so that equation (A1) reduces to

$$2 \zeta_s \int_0^{\omega_n T} (\dot{y})^2 d\tau = \mu \left(\frac{\omega_s}{\omega_n} \right)^2 \left\{ C_L Y \int_0^{2\pi} \sin(u + \varphi) \cos u du - C_R Y \int_0^{2\pi} \sin(u + \varphi_1) \cos u du \right\}, \quad u = \alpha \tau$$

or

$$2 \zeta_s \int_0^{\omega_n T} (\dot{y})^2 d\tau = \mu \left(\frac{\omega_s}{\omega_n} \right)^2 \left\{ \pi C_L Y \sin \varphi - \pi C_R Y \sin \varphi_1 \right\}. \quad (A2)$$

When equation (7) is evaluated in the same manner, one obtains

$$2 \zeta_s \int_0^{\omega_n T} (\dot{y})^2 d\tau = \mu \left(\frac{\omega_s}{\omega_n} \right)^2 \left\{ \int_0^{\omega_n T} C_{mh} \sin \alpha \tau \dot{y} d\tau - \int_0^{\omega_n T} C_{dh} \cos \alpha \tau \dot{y} d\tau \right\}. \quad (A3)$$

From the assumed solution to equation (7),

$$\dot{y} = \alpha Y \cos (\alpha \tau - \epsilon)$$

so that equation (A3) reduces to

$$2 \zeta_s \int_0^{\omega_n T} (\dot{y})^2 d\tau = \mu \left(\frac{\omega_s}{\omega_n} \right)^2 \left\{ C_{mh} Y \int_0^{2\pi} \sin u \cos (u - \epsilon) du - C_{dh} Y \int_0^{2\pi} \cos u \cos (u - \epsilon) du \right\}$$

or

$$2 \zeta_s \int_0^{\omega_n T} (\dot{y})^2 d\tau = \mu \left(\frac{\omega_s}{\omega_n} \right)^2 \left\{ \pi C_{mh} Y \sin \epsilon - \pi C_{dh} Y \cos \epsilon \right\}. \quad (A4)$$

A straight-forward comparison of equation (A4) with equation (A2) yields the results

$$C_L \sin \phi = - C_{dh} \cos \epsilon \quad \text{EXCITATION (10a)}$$

$$C_R \sin \phi_1 = - C_{mh} \sin \epsilon \quad \text{FLUID REACTION (DAMPING) (10c)}$$

as previously had been obtained. The "generalized Morison coefficient" C_{mh} from Sarpkaya's formulation [21], has a component $C_{mh} \sin \epsilon$ which acts to oppose the velocity \dot{y} of the structure (since ϵ is typically negative for vortex-excited, resonant oscillations) and acts effectively as a fluid reaction force as had been hypothesized by Griffin & Koopmann [19]. Likewise, the Morison coefficient C_{dh} , which is negative during vortex-excited oscillations, as shown in Figure 2, is in effect a lift force which transfers energy to the vibrating structure through the component $-C_{dh} \cos \epsilon$. This latter force is in phase with the velocity term \dot{y} . The results given by equations (A2) and (A4) show that the excitation force on the cylinder is balanced by a fluid reaction force and a structural damping force. The reaction or damping effect of the fluid can be measured simply in terms of an effective fluid damping factor ζ_F as shown in Figure 4, which is taken from the wind tunnel experiments with resonantly vibrating circular cylinders reported by Griffin & Koopmann [19]. Blake, Maga & Finkelstein [22] have made analogous measurements in a water tunnel with model hydrofoils which were resonantly excited by vortex shedding.

TABLE 1
 THE LIFT COEFFICIENTS OF VIBRATING CIRCULAR CYLINDERS;
 FROM GRIFFIN & KOOPMANN [19].

System	Damping coefficient, R_S (kg/sec)	Damping ratio, ζ_S	Mass ratio, μ	Reduced damping, $S_G = \zeta_S / \mu$	Response parameter, W^{++}
I	5×10^{-5}	6.8×10^{-4}	8.6×10^{-3}	0.079	0.068
II ⁺		3.3×10^{-4}	2.4×10^{-3}	0.14	0.033
III ⁺		1.6×10^{-4}	5.2×10^{-4}	0.31	0.016

⁺ Obtained by assuming $R_S = \text{constant}$ for all three systems. R_S for System I was measured directly in vacuo; see reference 1.

⁺⁺ $W = \frac{2 \alpha \zeta_S}{1 - \alpha^2}$, see equation (13c); data shown above correspond to the maximum amplitude \bar{Y}_{MAX} for each cylinder.

TABLE 2 (a)
HYDRODYNAMIC FORCES ON CIRCULAR CYLINDERS;
FROM SARPKAYA [21].

Displacement, $Y = Y/D$	Inertia Coefficient, C_{mh}	Drag Coefficient, C_{dh}	Reduced Velocity, $V_r = 5$.		Fluid Force Components, Equation (10) [†]	
			Phase Angle, $\beta = \arctan \left[\frac{C_{dh}}{C_{mh}} \right]$	Excitation, $-C_{dh} \cos \beta$	Damping, $-C_{mh} \sin \beta$	Inertia, $C_{dh} \sin \beta$
0.13	0.4	-0.2	-26.6°	0.18	0.18	0.089
0.25	0.4	-0.35	-41.2°	0.26	0.26	0.23
0.50	1.0 to 2.2	-0.9	-42° to 22.3°	0.67 to 0.83	0.67 to 0.83	0.60 to 0.34
0.75	1.0 to 2.6	-0.6	-28.8° to -11.9°	0.48 to 0.54	0.48 to 0.54	0.26 to 0.11

[†] $\epsilon = \beta + \gamma$ and $\gamma = \arctan \frac{2\alpha \tau_s}{1 - \alpha^2}$, where $W = \frac{w}{w_n}$, $\alpha = \frac{w}{w_n}$. In addition,

$W = 0.05$ is assumed (See Table 1).

^{††} The inertia coefficient is evaluated here in coordinates appropriate to a cylinder vibrating in a quiescent fluid or, equivalently, a fluid in uniform, steady motion.

TABLE 2(b)
ESTIMATED HYDRODYNAMIC FORCES ON CIRCULAR CYLINDERS;
 FROM MERCIER [20]

Reduced velocity, $V_r = 5.5-6$

Fluid Force Components, Equation (10)[†]

Displacement $Y = \bar{Y}/D$	Inertia Coefficient,		Drag Coefficient,		Phase angle,		Excitation,		Damping,		Inertia,	
	C_{mh}	C_{dh}	$\beta = \arctan\left(\frac{C_{dh}}{C_{mh}}\right)$	$\beta = \arctan\left(\frac{C_{dh}}{C_{mh}}\right)$	$-C_{dh} \cos \epsilon$	$-C_{mh} \sin \epsilon$	$-C_{dh} \cos \epsilon$	$-C_{mh} \sin \epsilon$	$C_{dh} \sin \epsilon$	$C_{dh} \sin \epsilon$	$C_{dh} \sin \epsilon$	$C_{dh} \sin \epsilon$
0.3	0.31	-0.32	-45.9°	-45.9°	0.23	0.21	0.23	0.21	0.22	0.22	0.22	0.22
0.5	0.51 to 1.23	-0.59	-49.1° to -25.6°	-49.1° to -25.6°	0.41 to 0.54	0.37 to 0.48	0.41 to 0.54	0.37 to 0.48	0.43 to 0.23	0.43 to 0.23	0.43 to 0.23	0.43 to 0.23
1.0	1.64	-0.13	-4.5°	-4.5°	0.13	0.047	0.13	0.047	0.0037	0.0037	0.0037	0.0037

[†] $\epsilon = \beta + \gamma$ and $\gamma = \arctan W$, where $W = \frac{2 \alpha \zeta_s}{1 - \alpha^2}$, $\alpha = \frac{w}{u}$. In addition,

$W = 0.05$ is assumed once again (See Table C1).

TABLE 3

THE LIFT COEFFICIENTS ON VIBRATING BLUFF CYLINDERS;
DESCRIPTION OF THE DATA IN FIGURE 6

<u>Symbol</u>	<u>Type of cylinder</u>	<u>Medium</u>	<u>Cylinder material</u>	<u>Investigator(s)</u>
▲	Flexible cantilever	Water	PVC	King
■			Aluminum Stainless steel	
●	Pivoted rigid cylinder	Water and Air	Brass	Vickery & Watkins
+	Spring-mounted rigid cylinder	Air	Aluminum tubing	Griffin & Koopmann
■	Rigid cylinder, forced oscillations	Water	Stainless steel	Mercier
○	Rigid cylinder, forced oscillations	Water	Aluminum tubing	Sarpkaya
△	Flexible cantilever	Air	Aluminum	Hartlen, Baines & Currie

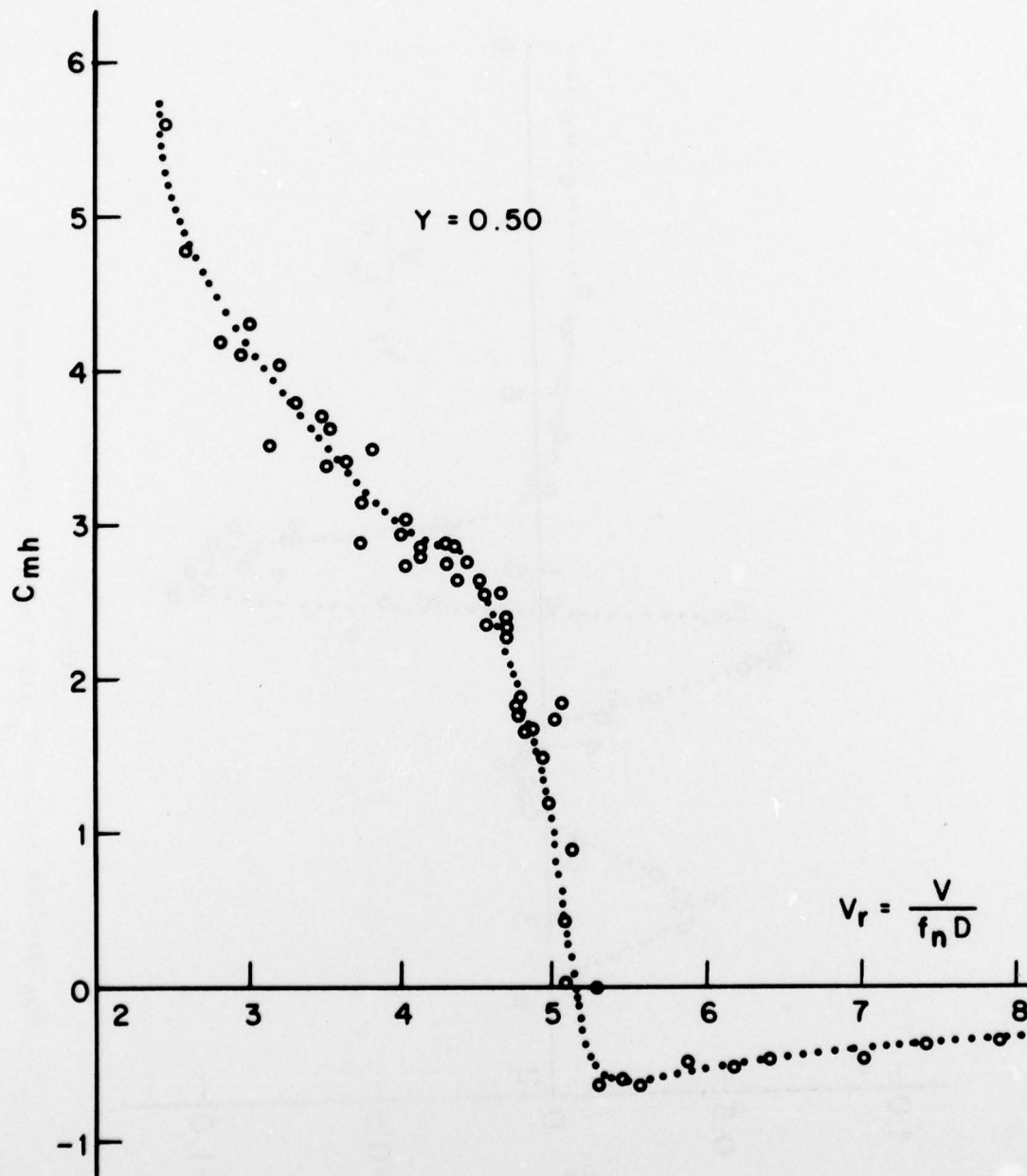


Figure 1
 C_{mh} plotted against V_r for $Y = 0.50$: from Sarpkaya [21].

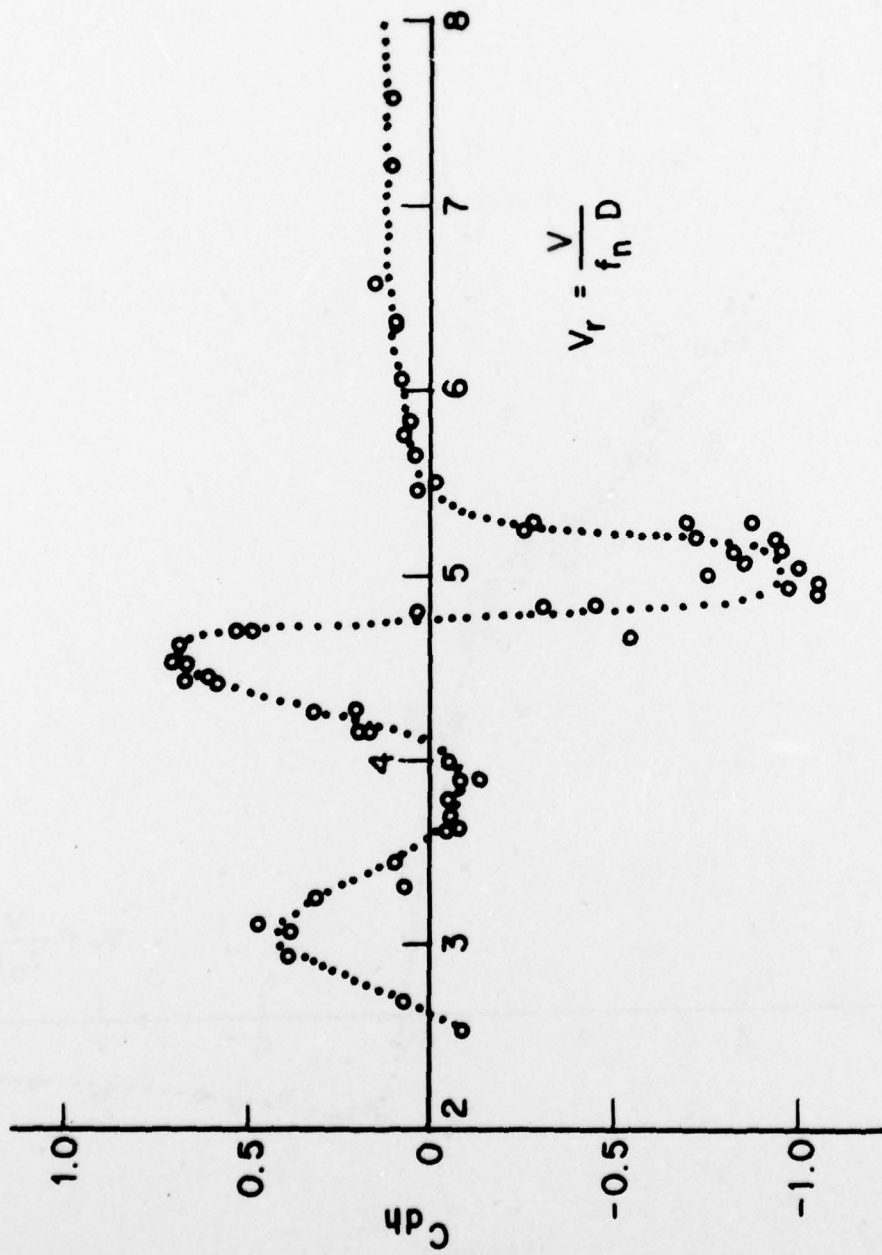


Figure 2
 C_{dh} plotted against V_r for $Y = 0.50$; from Sarpkaya [21].

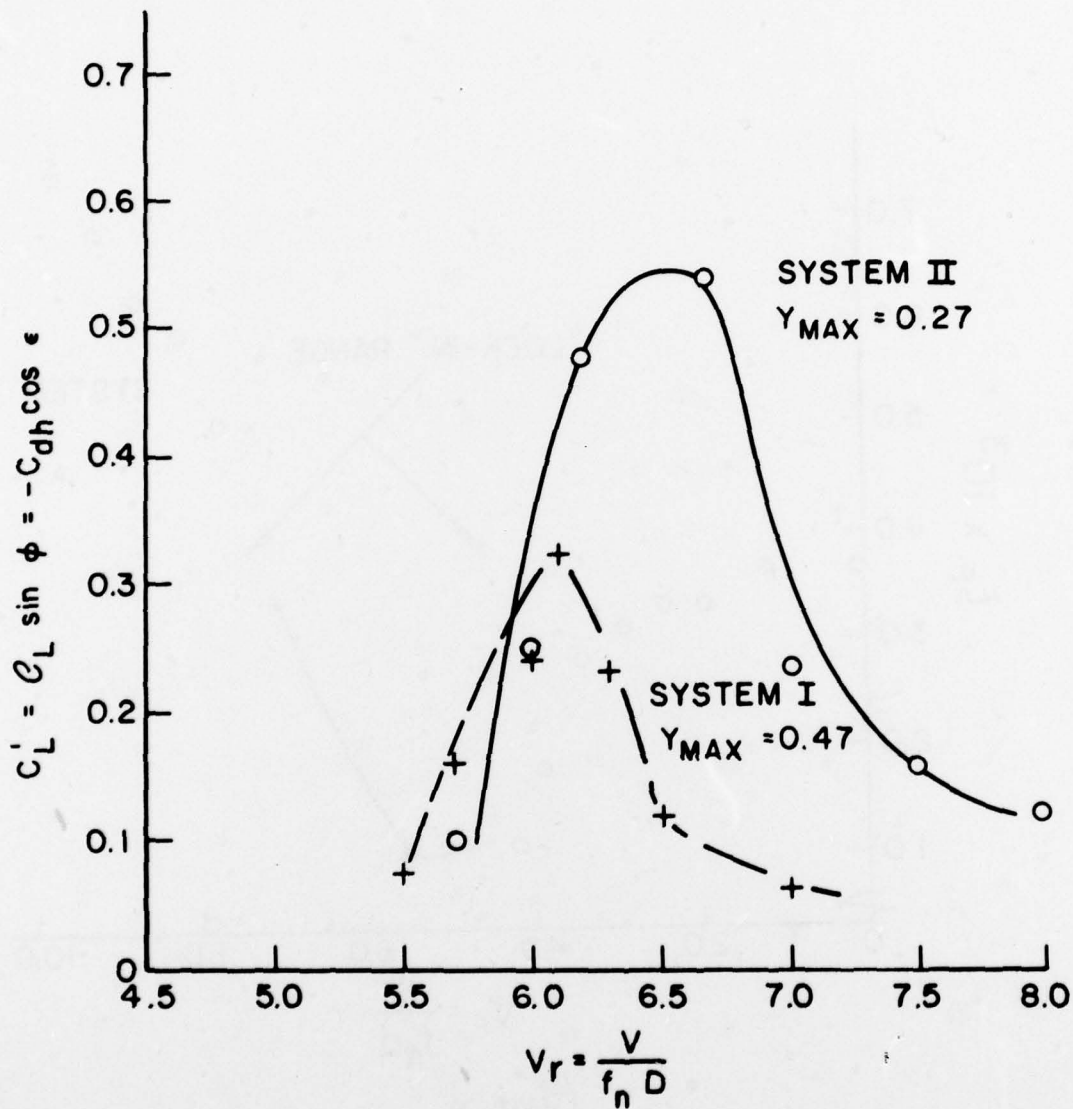


Figure 3

$C_L \sin \phi$ plotted against V_r for two cylinders (see Table 1) resonantly excited by vortex shedding; from Griffin & Koopmann [19].

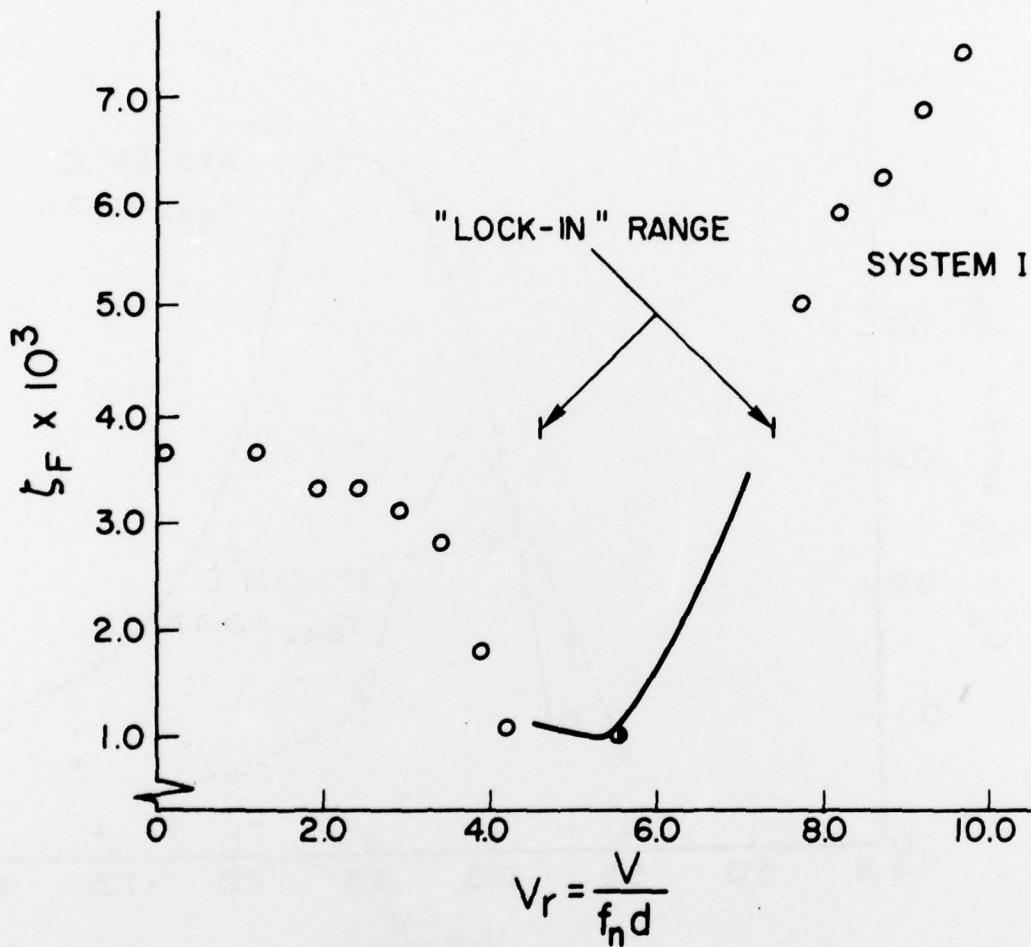
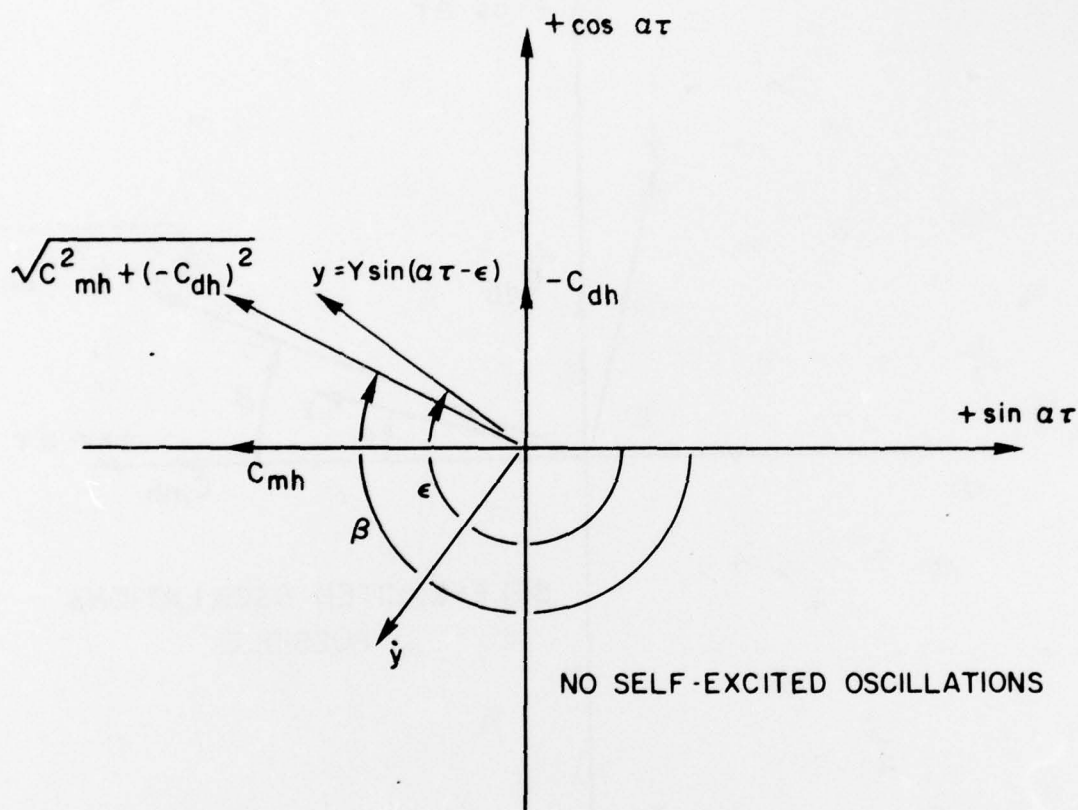


Figure 4

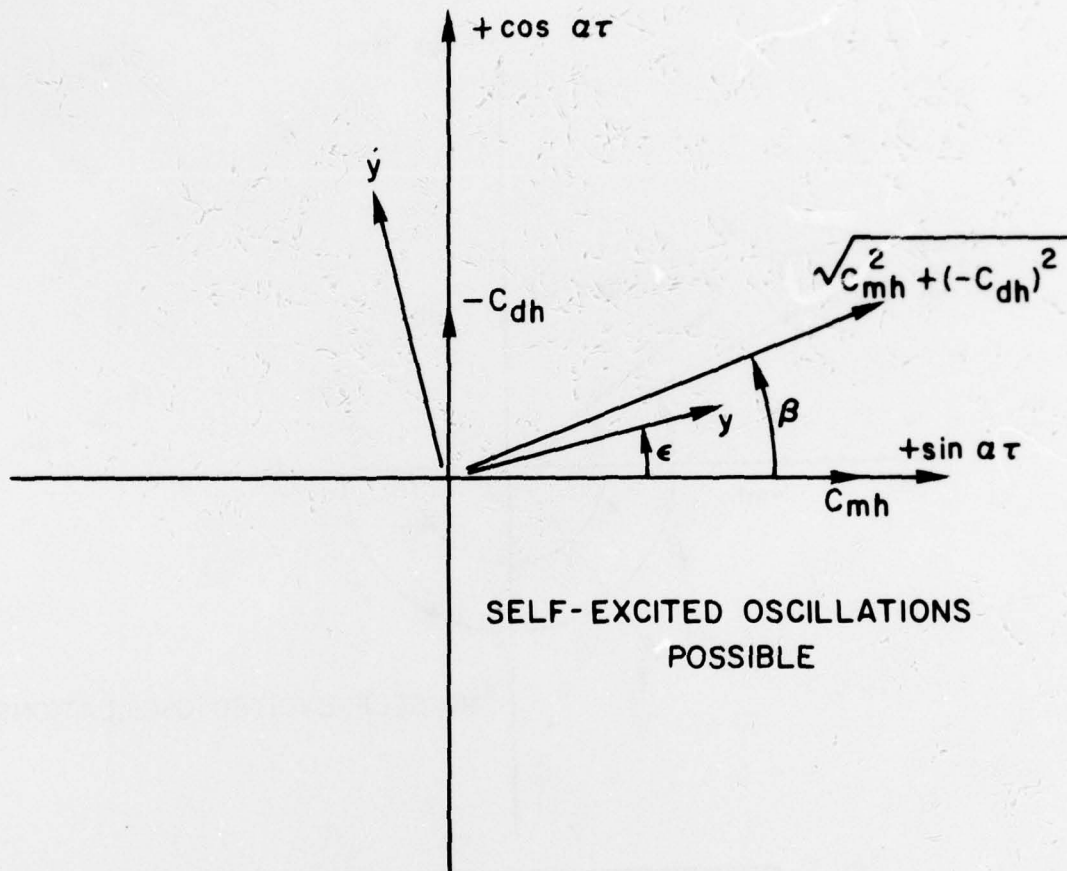
The fluid damping ratio ζ_F plotted against V_r ; from Griffin & Koopmann [19].



CASE 1: $Y = 0.25, V_r = 5.5$ $\begin{cases} C_{mh} = -0.5 \\ C_{dh} = -0.2 \end{cases}$
 $\epsilon = +204.7^\circ (W = 0.05)$
 $\beta = \text{ARC TAN}(C_{dh}/C_{mh}) = +201.8^\circ$

Figure 5(a)

Phase distribution of the flow-induced forces C_{mh} and C_{dh} , and the displacement y ; measured forces from Sarpkaya [21].



CASE 2: $\gamma = 0.50$, $V_r = 5$	$\begin{cases} C_{mh} = 1.6 \\ C_{dh} = -0.9 \end{cases}$
-------------------------------------	---

$$\epsilon = -26.5^\circ$$

$$\beta = \text{ARC TAN} (C_{dh}/C_{mh}) = -29.4^\circ$$

Figure 5(b)

Phase distribution of the flow-induced forces C_{mh} and C_{dh} , and the displacement y ; measured forces from Sarpkaya [21].

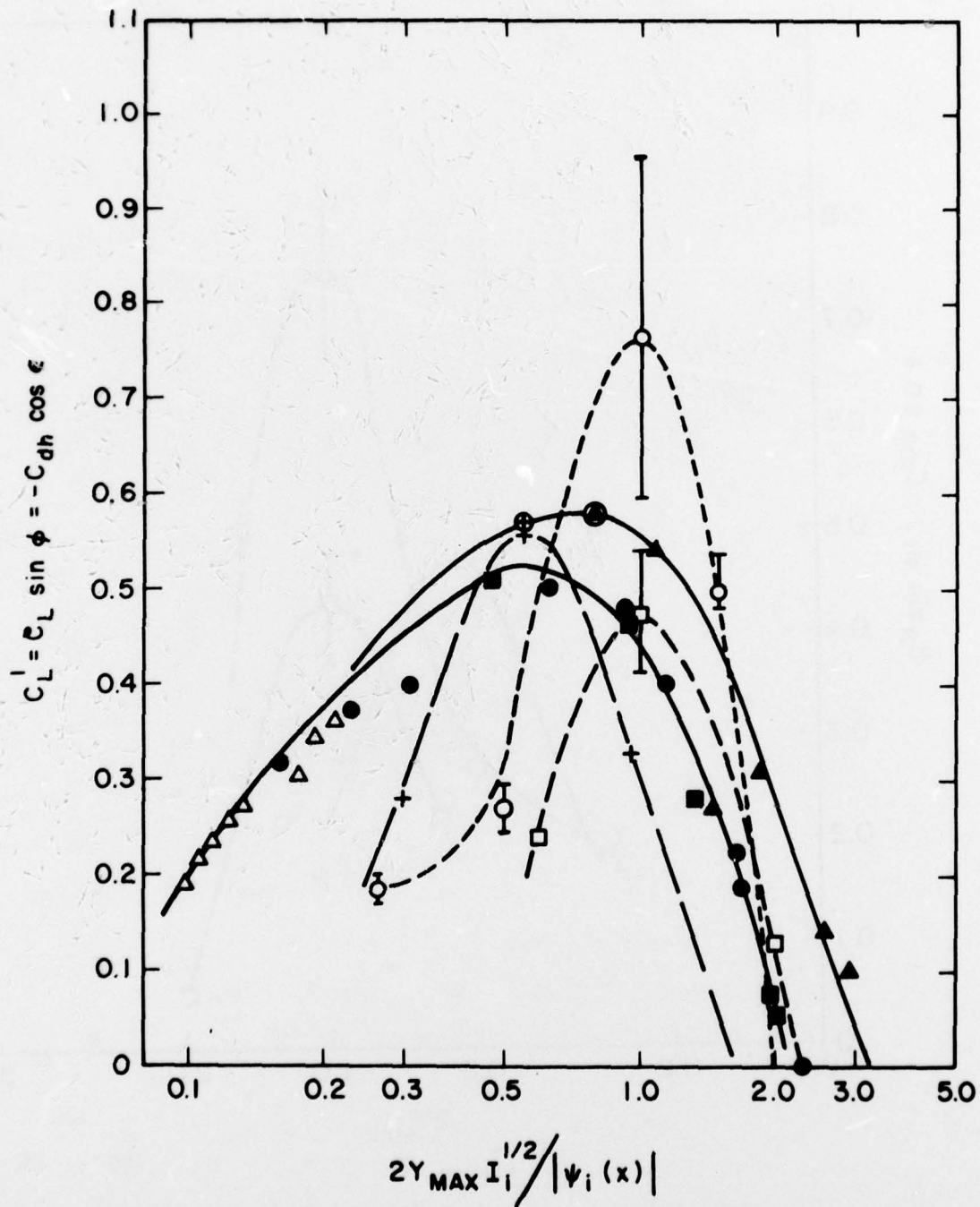


Figure 6

$C_L \sin \phi$ and $C_{dh} \cos \epsilon$ plotted against $2Y_{MAX}$ (scaled as shown); for legend see Table 3.

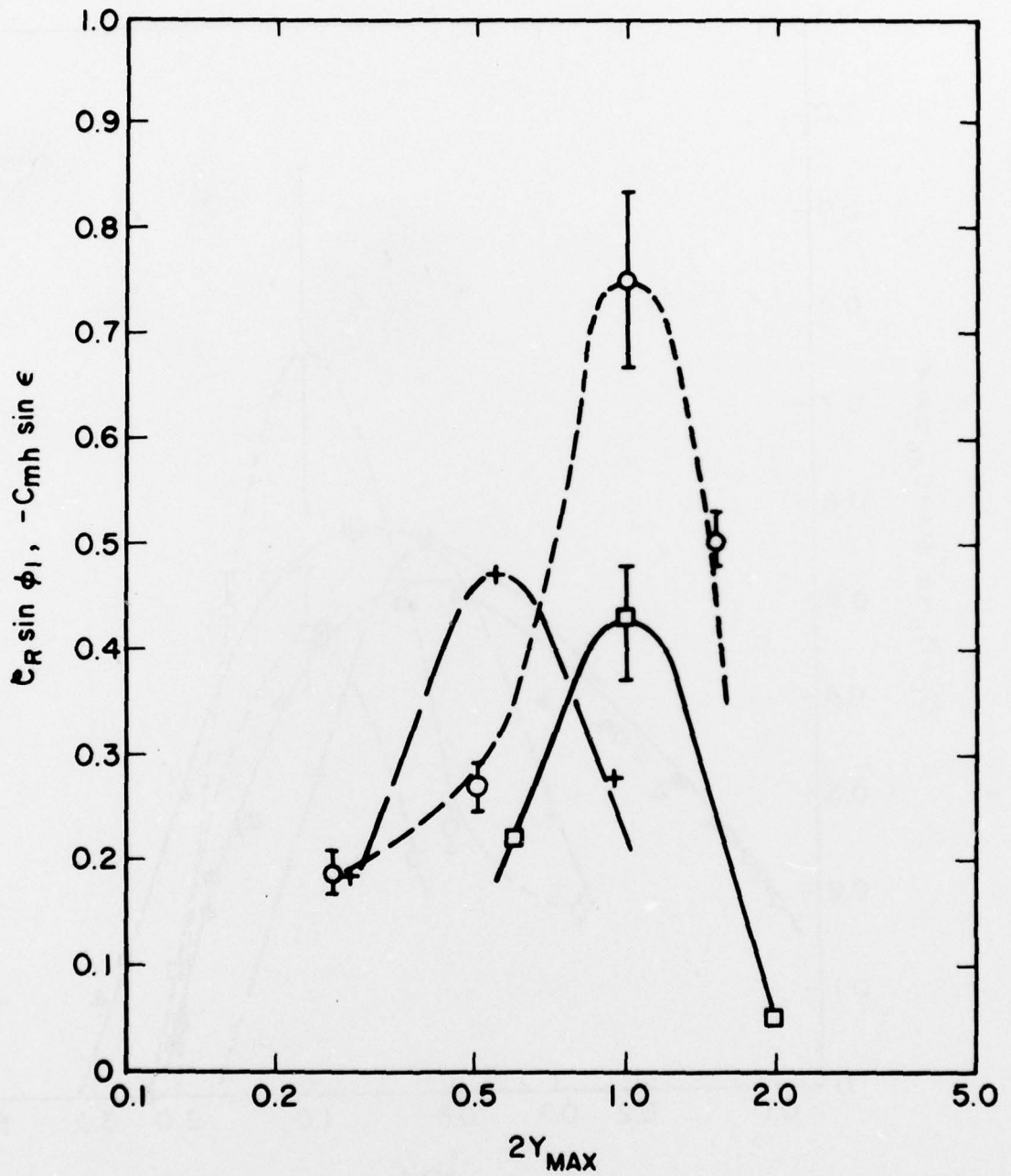


Figure 7

$C_R \sin \phi_1$ and $-C_{mh} \sin \epsilon$ plotted against $2Y_{MAX}$; from Griffin & Koopmann [19] - -; from Sarpkaya [21] ----; from Mercier [20] — (all circular cylinders).